

40.1: Invited Paper: The Zenithal Bistable Device: From concept to consumer

J. Cliff Jones

ZBD Displays Limited, Malvern Hills Science Park, Malvern, Worcs. WR13 5SZ, UK

Abstract

The first commercial use of the Zenithal Bistable Display (ZBD[®]) is for electronic point of purchase (epop[™]) signage in the retail sector. As a reflective bistable display, this novel LCD technology only consumes power if the image is updated. It is addressed using a simple passive matrix and consequently allows large amounts of information to be displayed using low cost STN drivers. The operating principles, manufacturing method and performance of ZBD are reviewed.

1. Introduction

The Zenithal Bistable Display (ZBD[®]) is the first commercially available LCD that uses surface bistability. It has the same basic construction as the conventional twisted-nematic display used in watches [1,2,3]. Instead of the rubbed polymer alignment layer usually used, one of the surfaces has a patterned or profiled surface designed to induce two or more alignment states. These states are retained indefinitely after being latched with an appropriate electrical signal. Because latching has a well defined threshold, the device can be addressed passively without cross talk. These properties make the devices ideal for low power applications where a high information content image is updated infrequently. Although, there is a number of potential device geometries, depending on the opposing surface [4], the present review will concentrate on the simple TN type geometry shown schematically in figure 1.

2. Obtaining Surface Bistability from Grating Alignment

Gratings have previously been used to impart monostable alignment to liquid crystals: with a local planar surface condition, the director lies parallel to the groove direction to minimise the elastic distortion energy. However, if the grating surface has a

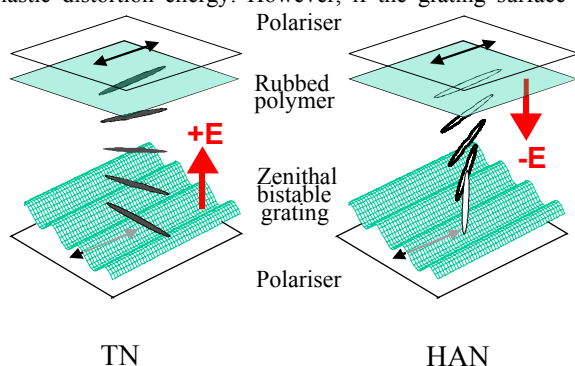


Figure 1 Schematic of the ZBD display.

local homeotropic condition (i.e. the director is normal to the surface at all points) then elastic deformation of the director field must occur. If the grating is shallow, the elastic deformation is small and the director remains in a Continuous state (figure 2a), with a uniform pretilt θ_C at some small distance from the grating that is close to 90° . If the grating is deep, the degree of elastic deformation is high, unless $+\frac{1}{2}$ and $-\frac{1}{2}$ defects form at the tops and bottoms of the grating grooves (figure 2b). The configuration in this Defect state leads to a low pretilt θ_D . The magnitude of θ_D is controlled by the relative position of the defects [4], and hence is dictated by the grating shape. An approximate relationship is:

$$\theta_D = \pi/2 - a\pi/L \quad (1)$$

where a is the distance between $+\frac{1}{2}$ and $-\frac{1}{2}$ defects and L is the distance between repeating defects (equal to the pitch for a periodic grating). Gratings with D state pretilts ranging from 0° to 55° have been produced in practice. For the ZBD devices operating in the TN mode, a pretilt of about 5° is ideal and so a near symmetric grating is used. Bistability results for a range of grating shapes between these extremes of C state stable shallow grating, and D state stable deep grating. Current production devices use a grating with $0.8\mu\text{m}$ pitch and $0.9\mu\text{m}$ amplitude.

The $+\frac{1}{2}$ and $-\frac{1}{2}$ defects annihilate close to the surface, at the boundary between high and low pretilt regions (that is black and white states, respectively). Such a C - D boundary is shown in figure 3.

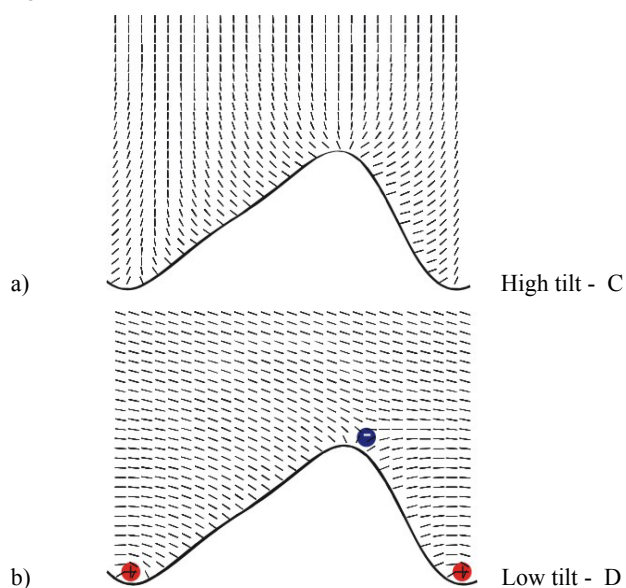


Figure 2 Bistable pre-tilts from a ZBD surface a) the Continuous C state; b) the Defect D state.

To ensure that bistability is maintained over the widest temperature range it is important that both states are retained even when one state is more energetically stable than the other. That is, a barrier to unwanted defect annihilation must be designed into the grating structure. One solution [5] is to use a 180° phase shift in the groove structure, as shown in figure 3. This “slip” acts both as pinning sites for these defect loops and as a nucleation site for the defect during the electro-optic response. Introducing slips into the grating design has enabled devices with good operating windows and shock stability to be maintained from temperatures below -10°C to above 70°C.

Bistability of this kind may occur for any surface that tends to stabilise defects. For example, a flat surface in which the local anchoring changes from planar to homeotropic may stabilise defects at the boundary between the regions of differing alignment. Either Defect or Continuous states may occur if the anchoring energies are weak. For a profiled surface, both C and D states can have the same energy at a single surface feature, such as an edge, isolated pillar or hole of the correct shape [6]. However, the use of a periodic or near periodic grating is advantageous, since it ensures uniform alignment (e.g. a constant pretilt angle for each of the two stable states) and constant latching voltages. Of course the grating shape may be varied over length scales much smaller than a pixel, to give analogue greyscale [7], or multi-domain structures. Alternatively, a random distribution of features may be used to vary the latching voltage and/or optical properties, for example to give a bistable scattering device [6].

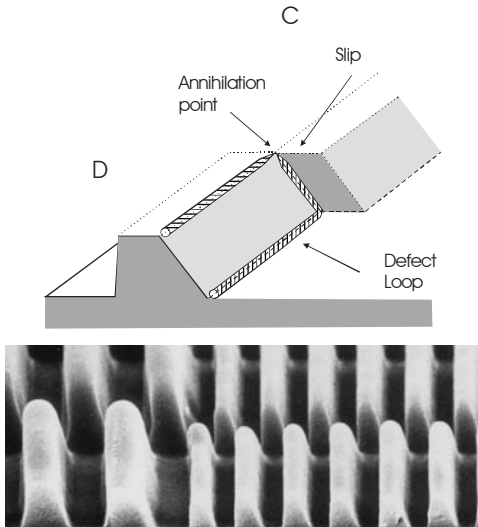


Figure 3. The use of grating slips to control nucleation and pinning of nematic ±½ defect lines at the top and bottom of the grating grooves.

3. A Polar Response to Applied Electric Fields

Key to ZBD operation is the ability to select one state or the other using electric pulses of opposite polarity [1]. The ZBD grating induces a surface polarisation in the liquid crystal and latching between the states is caused by the torque between this polarisation and an applied field. This polarisation is the result of the strong gradients in both the liquid crystal director field (flexoelectricity), and the order parameter (ordo-electricity). Despite

being present in all liquid crystal devices, these terms are usually considered negligible. For a deep sub-micron grating surface with strong local surface anchoring, these terms are much stronger than for conventional liquid crystal devices, allowing devices with 5µm cell gaps to be latched with pulses typically 10V and 250µs in duration [8]. The pulse duration required for latching τ has the approximate applied field dependence:

$$\tau \propto \frac{\gamma_1}{P_s E} \quad (2)$$

where γ₁ is the rotational viscosity and P_s is the surface polarisation associated with distortion of the liquid crystal director field close to the grating. Mixture B [8] latches at about 15V for a 500µs pulse at 23°C. Given γ₁ ≈ 0.25Nsm⁻² then the polarisation is approximately 0.2nCcm⁻².

Latching is controlled by a number of factors, including the various terms that contribute to the surface polarisation but also the dielectric effect of the grating material and ionic effects in response to the polar fields used. Figure 4 shows a typical plot of the latching characteristic for a 5.3µm TN mode device with Merck liquid crystal Mixture B at 23°C. The data are measured values for the D to C (■) and C to D (□) transitions in response to a symmetric bipolar pulse of duration 2τ and magnitude ±V. Note, regardless of geometry, a positive Δε liquid crystal tends to latch D for a positive voltage applied to the grating, and to the C state for the negative voltages. The diagram shows the voltage at which 50% of the cell is latched. The width of the transition from the first signs to complete latching is typically 8% of the latching voltage (i.e. about 1.2V).

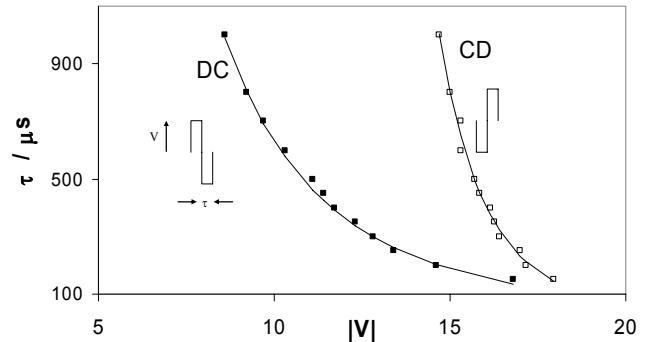


Figure 4. Bipolar pulse latching response for Mixture B at 23°C in a 5.3µm ZBD cell.

Also shown in figure 4 are straight line fits to the empirical expressions:

$$\tau_{CD} = \frac{A_i d}{(V - V_{th})^4} \quad (3)$$

$$\tau_{DC} = \frac{A_i d}{|V|^3} \quad (4)$$

$$A_i = \frac{\eta_i}{e_i P_s(T)} e^{\frac{U}{kT}} \quad i = DC, CD \quad (5)$$

$$V_{th} = B(T_m - T) \quad (6)$$

where d is the cell gap (plus $1.5\mu\text{m}$ to correct for the dielectric effect of the grating [8]), U is the activation energy, T_m is the monostable transition temperature and η_i are viscosity-like terms that include the effect of the surface anchoring energy, and e_i are constants that contains the appropriate scaling factors. For the fits shown, $d = 6.8\mu\text{m}$, $V_{th} = 9\text{V}$, $A_D = 1.1 \times 10^5 \text{V}^4\text{sm}^{-2}$ and $A_C = 9 \times 10^4 \text{V}^3\text{sm}^{-1}$. These expressions give a good description for all liquid crystal materials studied, cell gaps ranging from $2\mu\text{m}$ to $7\mu\text{m}$ and for different grating shapes. For example, figure 5 shows the cell gap dependence for $\tau = 500\mu\text{s}$ pulses for cells measured in the VAN geometry. This shows that latching is insensitive to variations in cell gap.

The V^{-3} dependence of τ_{DC} is due to the effect of the large positive $\Delta\epsilon$. The flexo-electric surface polarization is initially very weak and screened by mobile ions in the system. However, the flexo-electric polarization increases strongly with the director distortion from the normal dielectric effect on the director, which is proportional to $\Delta\epsilon V^2$. The V^{-4} dependence of τ_{CD} is more complex since it relates to the field-induced nucleation of defects at the top and bottom of the grating grooves, which in turn is dependent on the divergence of the field induced by the high dielectric mismatch between the grating material and liquid crystal.

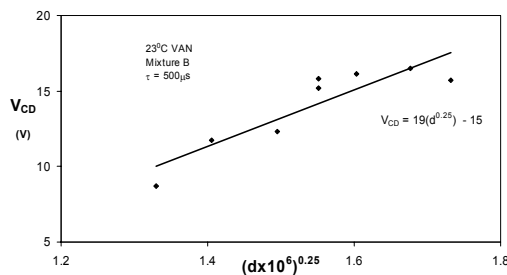


Figure 5. Typical cell gap dependence for V_{CD} .

The temperature dependence of the fitting parameters A_D and V_{th} are shown in figure 6. The threshold voltage has the fitting parameter $B = 0.18\text{V/K}$ using the measured monostable transition temperature of 75°C . For low temperatures (-20°C to 30°C) A_D follows a simple Arrhenius dependence (solid line in figure 6) with $U = 0.81\text{eV}$ and $\eta_D/e_D P_S = 2.5 \times 10^{-9} \text{V}^4\text{s}$.

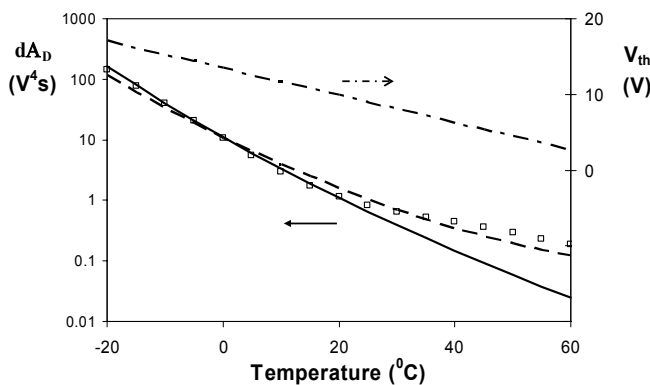


Figure 6. Temperature dependence of the V_{CD} fitting parameters.

At higher temperatures A_D has additional temperature dependences, associated with the change in magnitude of flexo-electric polarization and the effect of weak anchoring at higher temperatures. The dashed line shows the best fit where a term related to S^2 is included to mimic this behaviour (multiplying A_D by $0.1(1-T/T_{Ni})^{-1.7}$). The effect of varying anchoring energy on the latching voltages has been tested by varying the homeotropic material used for the grating surface. Although not measured directly, the anchoring is expected to be related to the surface energy: decreasing the surface energy (increasing contact angle) increases the latching voltage from C to D (V_{CD}) and decreases V_{DC} , as shown in figure 7.

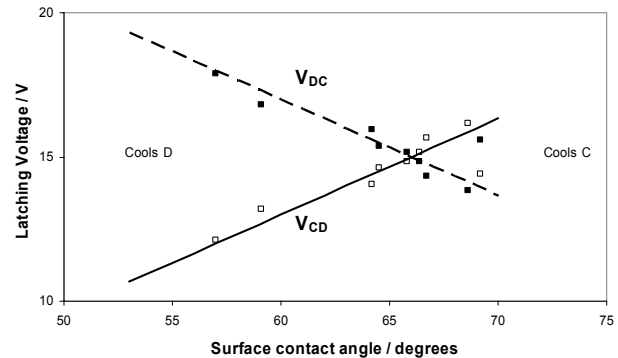


Figure 7 Typical latching voltages V_{CD} and V_{DC} versus grating surface contact angle (measured for mono-bromo-naphthalene, Mixture B at $500\mu\text{s}$).

4. Manufacturing and Addressing the Device

The profiled surface is manufactured easily and at low cost using a simple embossing technique. A master structure with the appropriate design is defined using conventional photolithography. This structure is first copied into nickel shims, and then into a roll of plastic film supplied to an LCD manufacturer. The original master structure (or its inverse) is then replicated in photo-polymer on the internal surface of the display by UV embossing. No additional costs arise for introducing complex surface profiles, since any increased complexity occurs in the formation of the original master grating only, and not the film. All other aspects of the LCD design are the same as for a conventional TN, and hence existing manufacturing lines are readily adapted to produce either conventional LCD or ZBD alongside each other.

Electrical addressing of the completed panel is done with conventional STN drivers. The display is addressed row-by-row, with a signal incorporating both an initial blanking portion that selects the C state, followed by a write signal that is synchronised with the data voltage applied to the columns [9]. A schematic of the row, column and resultant waveforms for the Progressive Line Blanking scheme is shown in figure 8. Note that, in practice, signals of opposite polarity are applied to both rows and columns, and these are inverted at each slot. This ensures that the drivers deliver the maximum voltage swing possible (i.e. $\pm V_{lcd}$). A typical addressing scheme would use $V_S = \pm 15\text{V}$, $V_D = \pm 3\text{V}$ with a 1ms per line pulse.

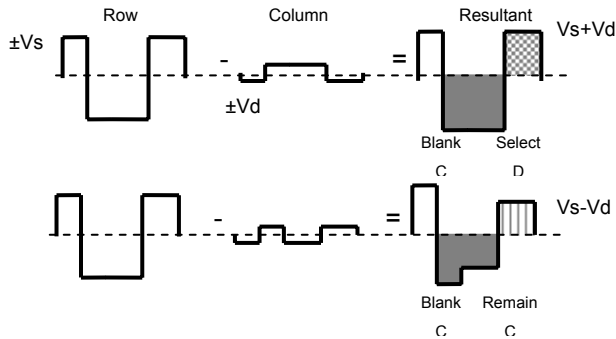


Figure 8 Addressing waveforms for Progressive Line Blanking. The grey shaded area has sufficient impulse to blank into the C state for either resultant. The final part of the resultant will either latch D (cross hatched) or be of insufficient impulse to latch D thereby retaining the C state (vertical shading).

5. Display Performance

ZBD Displays Limited has launched its epop™ product for retail signage applications based on the technology described here, figure 9. Pilots are underway in a number of leading retail and supermarket chains in Europe. The key attraction of the display for this market is display readability combined with the ability to update all product and promotional information remotely, whilst having a battery life that lasts for years despite the image being displayed constantly. A number of performance attributes for the current device are listed in Table 1.

Table 1 ZBD epop™ product performance

Property	Value
Image content	240 x 320
Display diagonal	102mm (4 inch)
Appearance	39% reflectivity 20: 1 contrast 160° Viewing angle (CR > 2)
Temperature range	0°C to 40°C
Storage temperatures	-20°C to + 70°C
Cell gap	5.3µm
Supply voltage	2.7V
Operating voltage	10V to 30V
Lifetime	> 1,000,000 updates > 10,000 hours at 90°C
Page update time	0.25 s at 20°C



Figure 9 ZBD® used in a retail signage application (epop™).

6. Conclusion

The potential of the ZBD device has begun to be realised with its first commercial application. This capitalises on a wealth of new technological advances, including understanding the relationship between grating shape and performance, the reproducible mass production of deep, sub-micron features on the inner surfaces of LCDs, and new liquid crystal material and addressing schemes that use the flexo-electric and ordo-electric effects in nematic liquid crystals. However, the flexibility of grating design promises to allow still further advances in the near term.

7. Acknowledgements

The author wishes to thank colleagues at ZBD displays, in particular Drs S. Beldon and R. Amos.

8. References

- [1] G.P. Bryan-Brown, C.V. Brown, J.C. Jones, (1995) *US patent 6,249,332*.
- [2] G.P. Bryan-Brown, C.V. Brown, J.C. Jones, E.L. Wood, I.C. Sage, P. Brett and J. Rudin, (1997) *SID Digest, Volume XXVIII, Boston, MA, USA, 5.3*, pp37 - 40.
- [3] J.C. Jones, G.P. Bryan-Brown, E.L. Wood, P. Brett, A. Graham and J.R. Hughes (2000) *Proceedings of SPIE, 3955*, 84 - 93.
- [4] J.C. Jones, (2006) *SID Digest, Volume XXXVII, Book 2, 51.2*, pp1626 - 29.
- [5] J.C. Jones (2003) *Patent Application WO 04,070,465*.
- [6] J.C. Jones (1999) *European Patent 1,234,207*
- [7] J.C. Jones, S. M. Beldon and E.L. Wood (2003) *J. SID. 11, 2*, pp 269- 275.
- [8] J.C. Jones, S. M. Beldon, P. Brett, M. Francis and M. Goulding (2003) *SID Digest, Volume XXXIV, Book 2 Boston, MA, USA, 26.3*, pp 954 - 957.
- [9] J.C. Jones (2000) *Patent Application WO 0,221,497*.